HHS Public Access

Author manuscript

Nat Methods. Author manuscript; available in PMC 2016 June 14.

Published in final edited form as:

Nat Methods. 2016 February ; 13(2): 147–150. doi:10.1038/nmeth.3691.

TRP channel mediated neuronal activation and ablation in freely behaving zebrafish

Shijia Chen[1,2], **Cindy N. Chiu**[1,2], **Kimberly L. McArthur**[3], **Joseph R. Fetcho**[3], and **David A. Prober**[1]

[1]Division of Biology and Biological Engineering, California Institute of Technology, Pasadena, CA, USA

[3]Department of Neurobiology and Behavior, Cornell University, Ithaca, NY, USA

The zebrafish has recently emerged as a useful vertebrate model system to study neural circuits and behavior, but tools to modulate neurons in freely behaving animals are limited. As a poikilotherm that lives in water, zebrafish are amenable to thermal and pharmacological perturbations. We exploit these properties by using transient receptor potential (TRP) channels to inducibly activate and ablate specific larval zebrafish (*Danio rerio*) neuronal populations using the chemical and thermal agonists of heterologously expressed TRPV1, TRPM8 and TRPA1.

Attempts to decipher neuronal mechanisms that regulate vertebrate behaviors are limited by the difficulty of manipulating mammalian neuronal circuits and the complexity of mammalian brains. The larval zebrafish has recently emerged as a model that overcomes these challenges due to several features, including transparency, lack of a mature blood brain barrier [1] and amenability to chemical and genetic perturbations [2]. Anatomical and molecular analyses have shown that zebrafish and mammalian brains are similar [3], so neuronal circuits that regulate zebrafish behaviors are likely to be conserved in mammals. However, use of zebrafish is limited by a paucity of validated tools to manipulate neuronal activity. Optogenetic tools that stimulate or inhibit neurons in response to light have been used to study restrained zebrafish larvae [4]. However, the light stimulus elicits a behavioral response in unrestrained larvae [5], which is problematic for many behavioral assays. The confounding effects of light can be avoided using tools that modulate neuronal activity in the presence of specific small molecules [6_8] or at specific temperatures [9], but these technologies have not been applied to zebrafish.

Corresponding author: ; Email: dprober@caltech.edu

[2]equal contribution

Author contributions

D.A.P. conceived of and supervised the project. S.C. and C.N.C. designed, performed, and analyzed all experiments, except physiology experiments, which were designed, performed and analyzed by K.L.M. and J.R.F. All authors collaborated to write the manuscript.

Competing financial interests

The authors declare no competing financial interests.

To develop these tools for use in freely swimming larval zebrafish, we tested three heterologous TRP channels that are activated by specific small molecules or temperatures. We tested rat TRPV1, which is activated by capsaicin (Csn) [10], rat TRPM8, which is activated by menthol [11], and rattlesnake TRPA1, which is activated at and above 28°C [12]. Importantly, the zebrafish TRPV1 ortholog is insensitive to Csn [13], zebrafish lack a TRPM8 ortholog, and the two zebrafish TRPA1 paralogs are not thermosensitive [14].

We used the *islet–1* sensory neuron enhancer to express TRP channels in trigeminal and Rohon–Beard sensory neurons (Fig. 1, Supplementary Figs. 1–3), and assayed for behavioral responses to channel agonists. Wild–type (WT) embryos did not respond to Csn (Supplementary Fig. 1c and Supplementary Video 1) [13], and TRPV1$^+$ embryos exhibited little locomotor activity when treated with vehicle or 0.1 μM Csn (Fig. 1b,c). However, exposure to 0.3 μM Csn or higher induced intense locomotor activity in transgenic embryos (Fig. 1b,c and Supplementary Video 1), consistent with activation of sensory neurons, and similar to the phenotype induced by channelrhodopsin–2 (ChR2) [4]. At 1 μM, Csn induced a response in 100% of embryos (Fig. 1b) consisting of 45 seconds of intense locomotor activity (Fig. 1c) and up to 2 hours of less intense activity (Supplementary Fig. 1c–e and Supplementary Video 2). These results suggest that Csn can activate TRPV1$^+$ neurons, and thus affect behavior, over long time periods. Following a 5 minute washout, reapplication of Csn elicited a similar behavioral response in 95% of embryos, indicating that the effect can be repeatedly induced. Similar responses were observed using increased temperature to activate TRPA1 and menthol to activate TRPM8 (Supplementary Figs. 2 and 3, Supplementary Videos 3 and 4).

To more directly test whether TRPV1$^+$ sensory neurons are activated by Csn, we assayed neuronal activity using *c–fos* fluorescent *in situ* hybridization (FISH) and *Tg(elavl3:GCaMP5G)* embryos, which express GCaMP5G in most post–mitotic neurons. We observed a dose–dependent increase in the number of *c–fos*–positive TRPV1$^+$ neurons (Fig. 1f,h), but no *c–fos* expression in WT siblings exposed to Csn (Fig. 1g,h) or in transgenic embryos exposed to vehicle (Fig. 1e,h). Consistent with these results, Csn induced a dose–dependent increase in GCaMP5G fluorescence in TRPV1$^+$ neurons (Supplementary Fig. 4). Exposure to 1 or 3 μM Csn induced transient GCaMP5G signals in 21% or 62% of TRPV1$^+$ neurons, respectively, with larger and longer effects at 3 μM Csn. At 10 μM Csn, 88% of TRPV1$^+$ neurons exhibited large increases in fluorescence that were sustained until Csn was washed out, which may have deleterious effects. No changes in GCaMP5G fluorescence were observed in controls. To determine whether TRPV1–induced calcium signaling is reversible, we exposed TRPV1–expressing embryos to 1 μM Csn, washed out the Csn, and then reapplied 1 μM Csn. Most cells that responded to the first application showed a similar response to the second application (Supplementary Fig. 5), indicating that Csn can reversibly and repeatedly stimulate TRPV1$^+$ neurons. Similar *c–fos* responses were observed using increased temperature and menthol to activate TRPA1 and TRPM8, respectively (Supplementary Figs. 2 and 3).

To confirm that observed calcium transients reflected Csn–evoked neuronal activity, we performed whole–cell patch clamp recordings from TRPV1$^+$ Rohon–Beard neurons in 2 days post–fertilization (dpf) embryos. Recordings from exposed spinal cord confirmed that

Csn depolarized the membrane potential and transiently increased excitability of TRPV1$^+$ neurons (Supplementary Fig. 6) but not TRPV1$^-$ neurons (data not shown). However, Csn failed to evoke action potentials, possibly because the sensory endings of Rohon–Beard neurons were damaged during surgery. We therefore performed recordings from intact spinal cord (Fig. 1i). We perfused 10 μM Csn into the recording chamber, although the Csn concentration increased gradually over several minutes as fluid was exchanged (see Online Methods). Prior to Csn exposure and during perfusion with vehicle, some Rohon–Beard neurons fired action potentials, probably stimulated by small movements of the microelectrode in the skin. In response to Csn (n = 6) but not DMSO (n = 3), TRPV1$^+$ neurons fired a prolonged burst of action potentials that began within 1–2 minutes (when Csn concentration was 1–5 μM) and tapered off over several minutes. Both the peak firing rate (Fig. 1i″) and average number of spikes (Supplementary Fig. 7a) were higher during Csn exposure. Resting membrane potential of the cell body depolarized only marginally (Supplementary Fig. 7b), indicating that Csn likely initiated action potentials by depolarizing the sensory endings. Thus, recordings from intact embryos support the conclusion that Csn increases neuronal activity in TRPV1$^+$ neurons.

We next tested the effect of prolonged activation of TRPV1 (Fig. 2). Using TRPV1–RFPT fluorescence as a proxy for cell number, we found that exposure to 1 μM Csn for 24 hours did not affect the number of TRPV1$^+$ neurons (Fig. 2b,d). However, these neurons were reduced by treatment with 10 μM Csn for 10 hours, and were essentially absent after 24 hours (Fig. 2c,d). Consistent with these observations, TRPV1$^+$ cells were TUNEL$^+$ when treated with 10 μM, but not 1 μM, Csn (Supplementary Fig. 8a–e). Neurons expressing EGFP alone were unaffected by exposure to 10 μM Csn for 24 hours (Supplementary Fig. 8f–h). TRPV1$^-$ embryos exposed to 10 μM Csn for up to 48 hours developed normally and exhibited normal locomotor activity. We conclude that strong and prolonged activation of TRPV1 results in apoptosis, allowing for targeted and inducible neuronal ablation. We did not observe neuronal ablation following prolonged activation of TRPA1 or TRPM8, likely because these channels induced weaker neuronal activity (Supplementary Figs 2 and 3) that was insufficient to induce excitotoxicity.

To determine whether TRP channels can be used to activate neurons deep within the brain, we expressed TRPV1 in hypothalamic neurons that express the neuropeptide hypocretin (Hcrt) (Supplementary Fig. 9a,b). We found that 1 μM and 10 μM Csn induced *c–fos* expression in 95% of Hcrt neurons (Fig. 3a,b,e,f,i), while little or no *c–fos* expression was observed in neighboring neurons that express the neuropeptide QRFP [15] (Fig. 3i, Supplementary Fig. 9g,h) or in Hcrt neurons of TRPV1$^-$ siblings (Fig. 3c,d,g,h,i). Similar to sensory neurons, high Csn levels ablated TRPV1$^+$ Hcrt neurons. At 10 μM Csn, over 50% of Hcrt neurons in *Tg(hcrt:EGFP);Tg(hcrt:TRPV1–RFPT)* larvae were absent after as little as 1 hour (Fig. 2e–g,q). This likely underestimates the number of ablated cells due to the persistence of EGFP, because immunohistochemical (IHC) detection of Hcrt showed loss of 80% of Hcrt neurons after treatment with 10 μM Csn for 24 hours (Fig. 2h,q). Exposure to 10 μM Csn for 24 hours had no effect on Hcrt neurons in *Tg(hcrt:EGFP)* larvae or on QRFP neurons in *Tg(qrfp:EGFP);Tg(hcrt:TRPV1–RFPT)* larvae (Fig. 2k,l,q). Treating *Tg(hcrt:EGFP);Tg(hcrt:TRPV1–RFPT)* larvae with 1 μM Csn, which induces *c–fos* expression, for 24 hours did not affect Hcrt cell number (Fig. 2m,q). TRPV1 is thus a single

tool with two applications: neuronal activation or ablation at low or high Csn levels, respectively.

Hcrt overexpression promotes locomotor activity and inhibits sleep in larval zebrafish [16]. Consistent with this result, activating Hcrt neurons using 1 μM Csn resulted in increased locomotor activity, decreased sleep, hyperactivity and fewer sleep bouts (Fig. 3j–m and Supplementary Fig. 9c,d). Conversely, ablating Hcrt neurons using 10 μM Csn resulted in decreased locomotor activity, increased sleep and more daytime sleep bouts (Fig. 3n–q and Supplementary Fig. 9e,f), similar to ablation of zebrafish Hcrt neurons using nitroreductase [17] and to narcolepsy, a disorder caused by reduced Hcrt neurons. Exposure to 10 μM Csn for over 48 hours had no effect on the health or behavior of WT larvae (Supplementary Fig. 10). Thus, TRPV1 can be used to manipulate neurons and affect behavior in freely behaving larvae.

TRP channels offer several advantages over alternative technologies (see Supplementary Discussion for comparison to similar tools). First, they can be used in freely behaving larvae without disrupting light–dependent behaviors. Second, because they do not require a light stimulus, they are compatible with bioluminescent and fluorescent neuronal activity reporters. Third, TRP channels conduct 1,000–fold more current than ChR2 [18], and thus can drive neuronal activity at lower expression levels. Fourth, our results suggest that TRPV1–mediated cell ablation may be faster and more robust than nitroreductase[17], although enhanced versions were recently reported [19, 20]. Fifth, the ability of the TRPV1 to activate or ablate neurons enables efficient screens for neurons that affect behavior. However, Csn concentrations that increase activity without causing ablation must be determined empirically for each cell type, as for other tools that manipulate neuronal activity [18]. Sixth, because different TRP channels are activated by distinct agonists, they can be used to simultaneously manipulate independent neuronal populations. We therefore expect that TRP channels will be useful tools for manipulating zebrafish neuronal circuits that control behavior.

Methods

Ethics statement

All experiments were performed using zebrafish (*Danio rerio*) larvae aged from 24 hpf to 7 dpf in accordance with the California Institute of Technology and Cornell University Institutional Animal Care and Use Committee guidelines.

Transgenic zebrafish

We fused rat TRPV1 (NM_031982), containing the E600K mutation that increases sensitivity to Csn by over 10–fold [21], rat TRPM8 (NM_134371), and *Crotalus atrox* (rattlesnake) TRPA1 (GU562967), to TagRFPT [22] at their C–termini. For expression in trigeminal and Rohon–Beard sensory neurons, we cloned the 4 kb *islet1* sensory neuron specific enhancer [23] upstream of the GAL4VP16 transcriptional activator [24], followed by 4xUAS:E1b minimal promoter–TRP channel–RFPT. We used the 1 kb zebrafish *hcrt* promoter [25] to express TRPV1–RFPT in Hcrt neurons. Each open reading frame was

followed by an SV40 polyA sequence and each cassette was flanked by ISce1 meganuclease sites and Tol2 transposase arms. We generated the *Tg(hcrt:TRPV1–RFPT)ct824* transgenic line using the Tol2 transposase method [26]. We generated the *Tg(islet1:GAL4VP16,4xUAS:TRPV1–RFPT)ct825* and *Tg(islet1:GAL4VP16,4xUAS:TRPA1–RFPT)ct826* transgenic lines using the ISce1 method [27]. TRPM8 experiments used transient injection of an *islet1:GAL4VP16,4xUAS:TRPM8–RFPT* transgene. The Tg(elavl3:GCaMP5G)a4598 [28], Et(e1b:GAL4VP16)s1102t [29], Tg(14xUAS:EGFP–Aequorin)a127 [30], Tg(–2.0Tru.Hcrt:EGFP)zf11Tg [16] and Tg(qrfp:EGFP)ct820 [15] transgenic lines have been described.

in situ hybridization and immunohistochemistry

We fixed zebrafish samples in 4% paraformaldehyde (PFA)/PBS for 12–16 hours at room temperature. We performed double fluorescent *in situ* hybridization (FISH) using digoxigenin (DIG) and 2,4–dinitrophenol (DNP)–labeled riboprobes and the TSA Plus DIG and DNP System (NEL747A001KT, PerkinElmer). We amplified an 818 bp template for the *c–fos* (also known as *fosab*, GenBank ID AL929435) probe from a larval zebrafish cDNA library using the primers 5′–CAGCTCCACCACAGTGAAGA–3′ and 5′–TGCAAACAATTCGCAAGTTC–3′. We amplified a 735 bp template for the *rfpt* probe from a TRPV1–RFPT plasmid using the primers 5′–ATGGTGTCTAAGGGCGAAGA–3′ and 5′–TTACTTGTACAGCTCGTCCATG–3′. We generated the *islet–1* probe as described [23] and performed immunohistochemistry as described [16]. Primary antibodies were chicken anti–GFP (1:500, GFP–1020, Aves), rabbit anti–tRFP (1:200, EVN–AB233–C100, Evrogen) and rabbit anti–orexin A (1:500, AB3704, Millipore). We used Alexa 488– and 568–conjugated secondary antibodies (1:500, Invitrogen). We mounted samples in 50% glycerol/PBS, and imaged them using a Zeiss LSM 780 laser–scanning confocal microscope with 488 nm and 561 nm lasers and 10x, 25x and 40x objectives. Numbers of samples analyzed in *hcrt:TRPV1–RFPT* cell activation experiment (Fig. 3a–k): 10 μM Csn, TRPV1$^+$, *hcrt:GFP* (n = 5); 10 μM Csn, TRPV1−, *hcrt:GFP* (n = 5); 1 μM Csn, TRPV1$^+$, *hcrt:GFP* (n = 5); 1 μM Csn, TRPV1−, *hcrt:GFP* (n = 2); 10 μM Csn, TRPV1$^+$, *qrfp:GFP* (n = 5). In Figures 2e–p and 3a–j, because we report the presence of labeled cells, and not the intensity of labeling within cells, we uniformly applied a gamma correction across all images to visualize cells with lower signal.

Small molecule treatment

We prepared frozen stock solutions of 100 mM Csn (M2028, Sigma) and 500 mM Menthol (M2772, Sigma) by dissolving the compounds in dimethyl sulfoxide (DMSO, 4948–02, Macron Chemicals). We prepared working concentrations just prior to embryo treatment by diluting the stock solutions into E3 medium (5 mM NaCl, 0.17 mM KCl, 0.33 mM $CaCl_2$, 0.33 mM $MgSO_4$, pH 7.4). All treatments contained a final concentration of 0.05% DMSO (*hcrt* experiments) or 0.2% DMSO (*islet1* experiments).

Temperature–dependent activation of TRPA1

We raised *Tg(islet1:Gal4VP16,UAS:TRPA1–RFPT)* larvae in E3 medium at 22.5°C or 26.5°C to avoid activating the TRPA1 channel. We transferred embryos to E3 medium at temperatures up to 28.5°C to activate the channel.

PSAM and DREADD experiments

DREADD—We transiently injected the following transgenes into WT embryos: *Tg(islet1:GAL4VP16,UAS:hM3Dq-RFPT)* and *Tg(islet1:GAL4VP16,UAS:rM3Ds-RFPT).* At 24 hpf, we immersed $RFPT^+$ embryos in 1 mg/ml, 500 μg/ml, 50 μg/ml, 25 μg/ml and 10 μg/ml clozapine-N-oxide but did not observe any behavioral responses. We also tested larvae transiently injected with *Tg(islet1:GAL4VP16,UAS:hM3Dq-RFPT)* at 4 dpf in 1 mg/ml and 300 μg/ml CNO. We did not observe any difference in behavior compared to mock injected WT larvae.

PSAM—We transiently injected the following transgenes into WT embryos: Tg(islet1:GAL4VP16,UAS:5HT3 HC Y115FL141F-2A-RFPT), Tg(islet1:GAL4VP16,UAS:5HT3 HC Y115FL141F-RFPT), Tg(islet1:GAL4VP16,UAS:RFPT-2A-5HT3 HC Y115FL141F). At 24 hpf, we immersed injected $RFPT^+$ embryos in 400 μM, 300 μM, 200 μM, 100 μM, 40 μM and 20 μM S89 (a gift from Scott Sternson, Janelia Farm) but did not observe any behavioral responses.

TRPV1–mediated cell ablation

For TRPV1–mediated Rohon–Beard cell ablation, we dechorionated 28 hpf embryos and treated them with 1 μM or 10 μM Csn for 24 hours. We imaged embryos just before Csn addition, and at 10 and 24 hours after Csn addition. At each time point, each embryo was anesthetized with 0.03% tricaine and oriented on its side. We acquired fluorescent images using a dsRed filter on a fluorescent stereomicroscope (M250c, Leica Microsystems Inc.) and a color CCD camera (DFC310FX, Leica Microsystems Inc.). We quantified fluorescence intensity using ImageJ in a 200 μm × 1.6 mm (28 hpf) or 100 μm × 2 mm (38 hpf and 52 hpf) region of interest that encompassed the dorsal spinal cord and most Rohon–Beard sensory neurons. We calculated fluorescence intensity by subtracting background fluorescence from the measured fluorescence.

For the TUNEL assay, we treated dechorionated 24 hpf embryos with vehicle, 1 μM or 10 μM Csn for 6 hours then fixed them in 4% PFA/PBS overnight at 4°C. Fixed embryos were dehydrated using methanol and stored at −20°C. Embryos were rehydrated using decreasing concentrations of methanol in PBST (PBS + 0.1% Tween), treated with 10 μg/ml proteinase K for 8 minutes, and fixed in 4% PFA/PBS for 20 minutes. Embryos were treated with 0.1% sodium citrate in PBST, then incubated with 90 μl labeling solution and 10 μl enzyme solution using the *In Situ* Cell Death Detection Kit, Fluorescein (11684795910, Roche) for one hour at 37°C. Embryos were washed three times with PBST and imaged using a Zeiss 780 confocal microscope with 25x water objective. The bright field overlay in Supplementary Figure 8a–d shows the position of Rohon–Beard neurons in the spinal cord.

Calcium Imaging

Embryos at 2 days post–fertilization (dpf) were paralyzed with 1 mg/ml α–bungarotoxin (2133, Fisher Scientific) dissolved in E3 medium, mounted on their side in 0.8% low melting point agarose in a 35 × 10 mm culture dish, and covered with 3 mL E3 medium. We imaged *Tg(elavl3:GCaMP5G)* fluorescence using a Zeiss 780 confocal microscope with a 20x water immersion objective. Samples were excited with a 488 nm laser and emitted light was collected through a 493–569 nm filter. We acquired images at 1 frame/second for 10 s before and 440 s after Csn administration. Frame acquisition time was approximately 900 ms. We added 1 mL of Csn at 4 μM, 12 μM, or 40 μM to the side of the culture dish to for a final concentration of 1 μM, 3 μM, or 10 μM, respectively. We measured fluorescence intensity by drawing regions of interest around Rohon–Beard neurons using ImageJ. We calculated change in fluorescence ($\Delta F/F_o$) as the fluorescence minus the initial fluorescence (defined as the mean fluorescence for the first 10 images) divided by initial fluorescence. To test whether TRPV1–induced calcium signaling is reversible, we performed calcium imaging as described above, except images were acquired for 10 s before and 290 s after adding 1 mL of 4 μM Csn to the side of the dish (final concentration = 1 μM). We then washed embryos three times for 5 minutes with E3 solution to remove Csn. The same embryos were then treated with Csn and imaged as described above.

Physiology

We performed whole–cell patch clamp recordings on 2 dpf *Tg(islet1:Gal4VP16,UAS:TRPV1–RFPT)* embryos. We paralyzed embryos in α–bungarotoxin (Biotoxins, Inc.; 1 mg/mL in purified water or 10% Hank's solution) and transferred them to a Sylgard–coated, glass–bottom specimen dish. Embryos were secured to the dish with custom etched tungsten pins through the notochord and covered with extracellular solution. For recordings from intact spinal cord, we immediately covered larvae with extracellular recording solution (in mM: 134 NaCl, 2.9 KCl, 1.2 $MgCl_2$, 10 HEPES, 10 glucose, 2.1 $CaCl_2$; adjusted to pH 7.8 with NaOH) and transferred them to the recording apparatus with no further dissection. For recordings from surgically dissected spinal cord, we first submerged larvae in 0.1% collagenase (Sigma) dissolved in extracellular recording solution. We removed the skin overlying the dorsal tail musculature with a sharp tungsten pin; after 10–15 min in collagenase, the blunt edge of the probe was used to gently abrade away the loosened muscle tissue to expose the spinal cord. We washed embryos 3x with fresh extracellular recording solution to remove collagenase and debris, then transferred them to the electrophysiological recording apparatus. Cells were visualized with an Olympus BX51WI inverted microscope equipped with infrared DIC optics, epifluorescence, and a 40x immersion objective, and were viewed with a CCD camera controlled by QCapture Pro 6.0 software (QImaging). We selected cells with moderate TRPV1–RFPT expression for recording; each cell was filled with fluorescent dye during recording (from the micropipette; see below) and imaged after recording to confirm neuron identity. We performed all experiments at room temperature.

We pulled micropipettes for whole–cell recording from thin–walled filamented capillary glass (A–M Systems) on a Flaming–Brown puller (Sutter Instruments), to a tip diameter of ~3–5 μm and resistance of 8–15 MΩ. We backfilled micropipettes with intracellular

recording solution (in mM: 125 K–gluconate, 2 $MgCl_2$, 10 HEPES, 10 EGTA, 4 Na_2–ATP; adjusted to pH 7.2 with KOH) containing 0.01% AlexaFluor 488 hydrazide fluorescent dye (Life Technologies). Micropipettes were advanced into the spinal cord using a motorized micro manipulator (MP–225, Sutter Instruments), under positive tip pressure (60 mmHg) maintained by a pneumatic transducer (DPM–1B, Bio–Tek Instruments). Once the tip was near the soma of the Rohon–Beard neuron, positive pressure was released to obtain a gigaohm seal to the cell membrane. A holding voltage of −65 mV was applied, and a sharp suction pulse ruptured the cell membrane to initiate whole–cell recording. We performed all recordings in current–clamp mode, where standard corrections were made for bridge balance and pipette capacitance.

Electrophysiological data were acquired with a MultiClamp 700A amplifier (Molecular Devices) and a Digidata 1322A digitizer (Molecular Devices), recorded with Clampex 8.2 software (Molecular Devices), and analyzed offline with Clampfit (Molecular Devices) and Matlab (Mathworks). Electrical signals from Rohon–Beard neurons were filtered at 30 kHz and digitized at 100 kHz (Rf = 500 MΩ). Access resistance was monitored periodically during recording and was typically less than 80 MΩ; in cases where access resistance did increase over time, gentle suction was used to unclog the tip and bring the access resistance back down to an acceptable value. All recorded neurons had stable resting membrane potentials between −40 and −70 mV. Since we were concerned primarily with changes in membrane potential and excitability (rather than absolute values), we have reported values as recorded without applying a correction for the junction potential, estimated to be 18.5 mV at 23°C.

We detected action potentials using a thresholding function, implemented in Clampex (Molecular Devices). We defined spike times by the peak of each action potential and converted to raster plots. We calculated average firing rate per unit time as the number of spikes fired over the course of an entire trial, divided by the length of that trial in minutes. To calculate peak firing rates, we convolved spike trains (1 ms bins) with a Gaussian kernel (sigma = 5 s), and determined the maximum value. We performed statistical analyses using Matlab (Mathworks). We used single depolarizing current pulses (50–300 pA) to coarsely determine the firing threshold of each neuron before Csn exposure. We used hyperpolarizing current pulses (10–40 pA) to determine the input resistance of neurons before and after Csn exposure (input resistance = steady–state change in membrane voltage/amplitude of applied current step; calculated as a linear fit to data points). We used repeated sets of depolarizing current pulses (25–400 mV, 200 ms each, 2s inter–stimulus interval) to probe changes in excitability during the depolarizing ramp response to Csn.

We applied Csn to the embryos in two ways. In perfusion experiments (used to collect data shown in Figure 1i and Supplementary Figures 5c and 6), Csn was pre–dissolved in extracellular recording solution (10 or 100 μM) and released into the dish (~1 mL/30 s) with simultaneous suction at the other side, such that the dish solution was replaced by the Csn solution over time. To estimate the dynamics of fluid exchange in the recording chamber during perfusion, we collected images as Fast Green dye (10 μM; Sigma) was perfused into the recording chamber, initially filled with water. As the concentrated dye mixed with the chamber solution, the mean luminance of the chamber images decreased over time. We

collected images at 20 second intervals for 10 minutes, then used the time course of decreasing mean luminance to estimate how long it took for the dye concentration in the chamber to reach 10% and near 100% of the maximum dye concentration. Based on our observations, we estimate that the concentration of Csn in the chamber reached 10% of maximum within the first minute of perfusion and would reach near 100% of maximum only after 10 minutes of perfusion. For a subset of wash–out experiments, we replaced the Csn solution over time with fresh extracellular solution, and we repeated membrane potential, spiking threshold, and input resistance measurements following several minutes of perfusion with the wash–out solution. In diffusion experiments, we released concentrated Csn (100 mM in DMSO) through a broken–off recording pipette positioned at the edge of the recording dish (final concentration of 100 μM in extracellular recording solution).

Locomotor activity behavioral assay

We raised larval zebrafish on a 14 hour:10 hour light:dark cycle at 28.5°C (or 22°C for *Tg(islet1:GAL4VP16,UAS:TRPA1–RFPT)* larvae) with lights on at 9 am and off at 11 pm. We placed individual larvae into each well of a 96–well plate (7701–1651, Whatman) containing 650 μL E3 embryo medium. In most experiments, we sealed plates with an optical adhesive film (4311971, Applied Biosystems) to prevent evaporation. The introduces air bubbles in some which occlude tracking of larvae and are discarded from analysis. In *islet1* experiments, we transferred 2 dpf larvae into E3 medium containing Csn or DMSO vehicle control immediately before the start of behavioral recording at 12 pm. In *hcrt* experiments, we transferred 5 dpf larvae into E3 medium containing Csn 1 hour before the start of behavioral recording at 11 pm. We monitored locomotor activity using an automated videotracking system (Viewpoint Life Sciences) with a Dinion one–third inch monochrome camera (Dragonfly 2, Point Grey) fitted with a variable–focus megapixel lens (M5018–MP, Computar) and infrared filter. We recorded the movement of each larva at 15 Hz, with an integration time of 1 s for *islet1* experiments and 1 min for *hcrt* experiments, using the quantization mode. The 96–well plate and camera were housed inside a custom–modified Zebrabox (Viewpoint Life Sciences) that was continuously illuminated with infrared lights and illuminated with white lights from 9 am to 11 pm. The 96–well plate was housed in a recirculating water chamber to maintain a constant temperature of 28.5°C (or 25.5°C for *Tg(islet1:GAL4VP16,UAS:TRPA1–RFPT)* larvae). The parameters for detection were: detection threshold, 15; burst, 29; freeze, 3. We processed data using custom PERL and Matlab (Mathworks) scripts. We performed statistical tests using JMP (SAS) and Matlab (Mathworks). In figures showing behavioral data, activity refers to the average amount of locomotor activity of all animals of a particular genotype or condition during the indicated time interval. It was previously shown that zebrafish larvae that are inactive for one or more minutes exhibit an increased arousal threshold, indicating that one or more minutes of inactivity is a sleep–like state [16, 17]. Thus, sleep refers to larvae that are inactive for one or more continuous minutes. Exposure to 10 μM Csn for over 48 hours had no obvious effect on larval health, as determined by morphological observation, behavioral responses to acoustic and mechanical stimuli, and locomotor activity levels.

Statistical Analyses

For *c–fos* FISH, GCaMP5G, cell ablation and behavioral data, we used the Wilcoxon rank–sum test for pairwise comparisons, and the Kruskal–Wallis test followed by the Steel–Dwass test for analyses involving multiple comparisons. To compare peak and average firing rates recorded during perfusion of DMSO vehicle alone and 10 μM Csn, we performed one–tailed Wilcoxon rank sum tests to test the hypothesis that firing rates were significantly higher with Csn than with DMSO vehicle. For experiments in involving quantification, samples were genotyped following analysis, and thus were scored in a blind fashion.

Supplementary Material

Refer to Web version on PubMed Central for supplementary material.

Acknowledgments

We thank A. Chen, A. Cruz, A. Dominguez, J. Engle, S. Khan, K. Molinder, B. Niles, V. Sapin and L. Wang for technical assistance. This work was supported by grants from the US National Institutes of Health (F31–NS07842A to SC; F32–NS083099 to K.L.M; R01–NS26539 and DP1–OD006411 to J.R.F; R00–NS060996, R01–NS070911 and R01–DA031367 to D.A.P.) and the Mallinckrodt Foundation, the Rita Allen Foundation and the Brain and Behavior Research Foundation (D.A.P.).

References

1. Fleming A, Diekmann H, Goldsmith P. Functional characterisation of the maturation of the blood-brain barrier in larval zebrafish. PLoS ONE. 2013; 8:e77548. [PubMed: 24147021]
2. Wolman M, Granato M. Behavioral genetics in larval zebrafish: learning from the young. Dev Neurobiol. 2012; 72:366–372. [PubMed: 22328273]
3. Chiu CN, Prober DA. Regulation of zebrafish sleep and arousal states: current and prospective approaches. Front Neural Circuits. 2013; 7:58. [PubMed: 23576957]
4. Douglass AD, Kraves S, Deisseroth K, Schier AF, Engert F. Escape behavior elicited by single, channelrhodopsin-2-evoked spikes in zebrafish somatosensory neurons. Curr Biol. 2008; 18:1133–1137. [PubMed: 18682213]
5. Zhu P, et al. Optogenetic Dissection of Neuronal Circuits in Zebrafish using Viral Gene Transfer and the Tet System. Front Neural Circuits. 2009; 3:21. [PubMed: 20126518]
6. Arenkiel BR, Klein ME, Davison IG, Katz LC, Ehlers MD. Genetic control of neuronal activity in mice conditionally expressing TRPV1. Nat Methods. 2008; 5:299–302. [PubMed: 18327266]
7. Alexander GM, et al. Remote control of neuronal activity in transgenic mice expressing evolved G protein-coupled receptors. Neuron. 2009; 63:27–39. [PubMed: 19607790]
8. Magnus CJ, et al. Chemical and genetic engineering of selective ion channel-ligand interactions. Science. 2011; 333:1292–1296. [PubMed: 21885782]
9. Hamada FN, et al. An internal thermal sensor controlling temperature preference in Drosophila. Nature. 2008
10. Caterina MJ, et al. The capsaicin receptor: a heat-activated ion channel in the pain pathway. Nature. 1997; 389:816–824. [PubMed: 9349813]
11. Peier AM, et al. A TRP channel that senses cold stimuli and menthol. Cell. 2002; 108:705–715. [PubMed: 11893340]
12. Gracheva EO, et al. Molecular basis of infrared detection by snakes. Nature. 2010; 464:1006–1011. [PubMed: 20228791]
13. Gau P, et al. The zebrafish ortholog of TRPV1 is required for heat-induced locomotion. J Neurosci. 2013; 33:5249–5260. [PubMed: 23516290]

14. Prober DA, et al. Zebrafish TRPA1 channels are required for chemosensation but not for thermosensation or mechanosensory hair cell function. J Neurosci. 2008; 28:10102–10110. [PubMed: 18829968]
15. Liu J, et al. Evolutionarily conserved regulation of hypocretin neuron specification by Lhx9. Development. 2015; 142:1113–1124. [PubMed: 25725064]
16. Prober DA, Rihel J, Onah AA, Sung RJ, Schier AF. Hypocretin/orexin overexpression induces an insomnia-like phenotype in zebrafish. J Neurosci. 2006; 26:13400–13410. [PubMed: 17182791]
17. Elbaz I, Yelin-Bekerman L, Nicenboim J, Vatine G, Appelbaum L. Genetic ablation of hypocretin neurons alters behavioral state transitions in zebrafish. J Neurosci. 2012; 32:12961–12972. [PubMed: 22973020]
18. Bernstein JG, Garrity PA, Boyden ES. Optogenetics and thermogenetics: technologies for controlling the activity of targeted cells within intact neural circuits. Curr Opin Neurobiol. 2012; 22:61–71. [PubMed: 22119320]
19. Mathias JR, Zhang Z, Saxena MT, Mumm JS. Enhanced cell-specific ablation in zebrafish using a triple mutant of Escherichia coli nitroreductase. Zebrafish. 2014; 11:85–97. [PubMed: 24428354]
20. Tabor KM, et al. Direct activation of the Mauthner cell by electric field pulses drives ultra-rapid escape responses. J Neurophysiol. 2014
21. Jordt SE, Tominaga M, Julius D. Acid potentiation of the capsaicin receptor determined by a key extracellular site. Proc Natl Acad Sci U S A. 2000; 97:8134–8139. [PubMed: 10859346]
22. Shaner NC, et al. Improving the photostability of bright monomeric orange and red fluorescent proteins. Nat Methods. 2008; 5:545–551. [PubMed: 18454154]
23. Higashijima S, Hotta Y, Okamoto H. Visualization of cranial motor neurons in live transgenic zebrafish expressing green fluorescent protein under the control of the islet-1 promoter/enhancer. J Neurosci. 2000; 20:206–218. [PubMed: 10627598]
24. Koster RW, Fraser SE. Tracing transgene expression in living zebrafish embryos. Dev Biol. 2001; 233:329–346. [PubMed: 11336499]
25. Faraco JH, et al. Regulation of hypocretin (orexin) expression in embryonic zebrafish. J Biol Chem. 2006; 281:29753–29761. [PubMed: 16867991]
26. Kawakami K. Transposon tools and methods in zebrafish. Dev Dyn. 2005; 234:244–254. [PubMed: 16110506]
27. Thermes V, et al. I-SceI meganuclease mediates highly efficient transgenesis in fish. Mech Dev. 2002; 118:91–98. [PubMed: 12351173]
28. Ahrens MB, Orger MB, Robson DN, Li JM, Keller PJ. Whole-brain functional imaging at cellular resolution using light-sheet microscopy. Nat Methods. 2013; 10:413–420. [PubMed: 23524393]
29. Scott EK, Baier H. The cellular architecture of the larval zebrafish tectum, as revealed by gal4 enhancer trap lines. Front Neural Circuits. 2009; 3:13. [PubMed: 19862330]
30. Naumann EA, Kampff AR, Prober DA, Schier AF, Engert F. Monitoring neural activity with bioluminescence during natural behavior. Nat Neurosci. 2010; 13:513–520. [PubMed: 20305645]

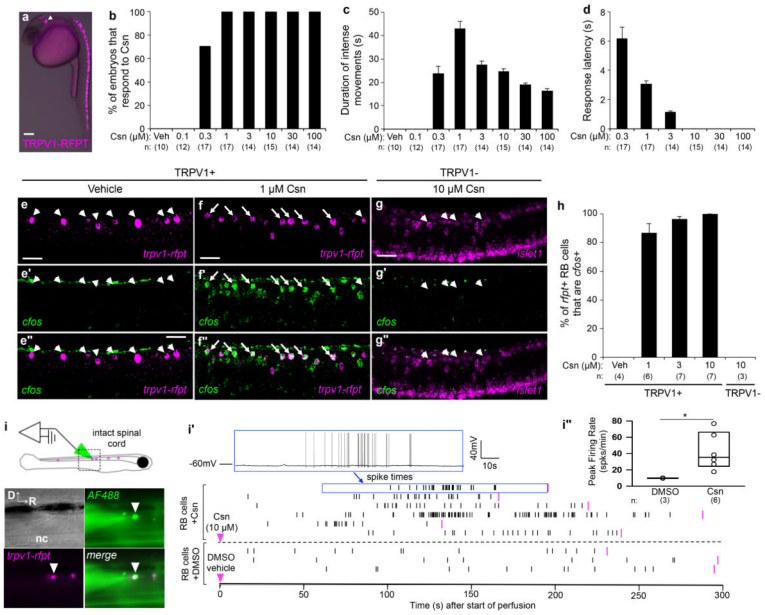

Figure 1. Csn induces locomotor and neuronal activity in embryos expressing TRPV1 in sensory neurons

A 24 hours post–fertilization (hpf) *Tg(islet1:GAL4VP16,UAS:TRPV1–RFPT)* embryo exhibits RFPT fluorescence in trigeminal (arrowhead) and Rohon–Beard sensory neurons [(a) and Supplementary Fig. 1a,b]. (b–d) 24 hpf transgenic embryos exhibited a dose–dependent locomotor response to Csn, (b–d). Mean ± s.e.m. is shown (c,d). This response ceased immediately upon removal from the Csn solution (not shown). WT siblings did not respond to Csn at any tested concentration (Supplementary Fig. 1c–e and Video 1). (e–g) Representative double FISH images. *c–fos* expression was induced in TRPV1–RFPT^{+} Rohon–Beard neurons in embryos exposed to 1 μM Csn for 45 minutes (f), but not in transgenic siblings exposed to vehicle control (e) or WT siblings exposed to 10 μM Csn (g). *islet1* expression identified Rohon–Beard neurons in WT embryos (g). Arrows and arrowheads indicate Rohon–Beard neurons that did and did not express *c–fos*, respectively. (h) Mean ± s.e.m. percentage of TRPV1–RFPT^{+} Rohon–Beard neurons that expressed *c–fos*. (i) Whole–cell recording data in intact 2 dpf *Tg(islet1:GAL4VP16,UAS:TRPV1–RFPT)* embryos. The white arrowhead indicates a TRPV1^{+} Rohon–Beard neuron that was filled with Alexa Fluor 488 (AF488) during recording. A sample membrane potential trace for this neuron is shown (blue inset, i′). Spike times were converted to raster plots for embryos perfused with DMSO vehicle ($n = 3$) and 10 μM Csn ($n = 6$). Magenta arrowheads indicate the start of perfusion and magenta bars in each raster indicate the end of recording for that neuron during that experimental condition. Peak firing rate was significantly higher during perfusion of Csn than DMSO (i″; *$P = 0.0119$ by Wilcoxon rank–sum test). nc = notochord.

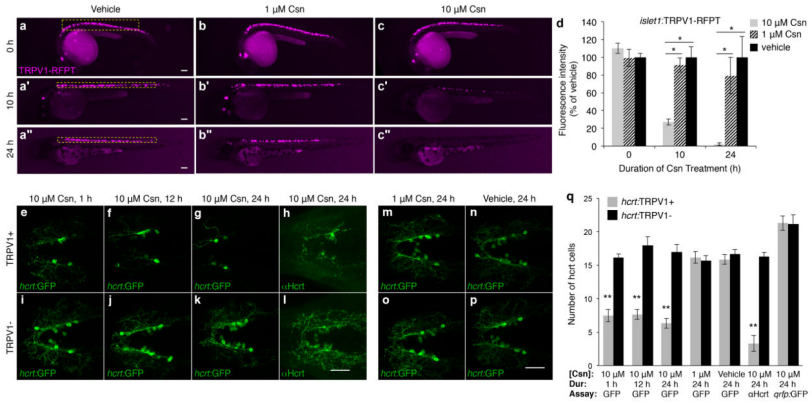

Figure 2. Csn dose–dependent ablation of TRPV1–expressing neurons

(a–c) Representative images of *Tg(islet1:GAL4VP16,UAS:TRPV1–RFPT)* embryos incubated in vehicle, 1 μM Csn or 10 μM Csn starting at 28 hpf. RFPT fluorescence was reduced and essentially absent after 10 h and 24 h, respectively, in 10 μM Csn, (c). Incubation in 1 μM Csn had no effect on RFPT fluorescence (b) compared to vehicle (a). (d) Mean ± s.e.m. RFPT fluorescence intensity for the conditions shown in (a–c). (e–q) Representative images of Hcrt neurons, detected by anti–EGFP IHC in *Tg(hcrt:TRPV1–RFPT)*;*Tg(hcrt:EGFP)* (e–g,m,n) or *Tg(hcrt:EGFP)* (i–k,o,p) larvae. Hcrt protein was detected by IHC in *Tg(hcrt:TRPV1–RFPT)* (h) or WT (l) siblings. Dorsal views of 5 dpf larval brains with rostral at left are shown. Images are maximum intensity projections of 40 μm confocal z–stacks. A gamma correction was uniformly applied across all images to visualize cells with lower signal in panels (e–p). (q) Mean ± s.e.m. number of cells for the conditions shown in (e–p). Six animals were analyzed for each condition (d,q). **P*<0.05 and ***P*<0.01 by the Kruskal–Wallis test followed by the Steel–Dwass test to correct for multiple comparisons (d) and the Wilcoxon rank–sum test (q). Scale = 100 μm (a–a″) and 20 μm (l,p).

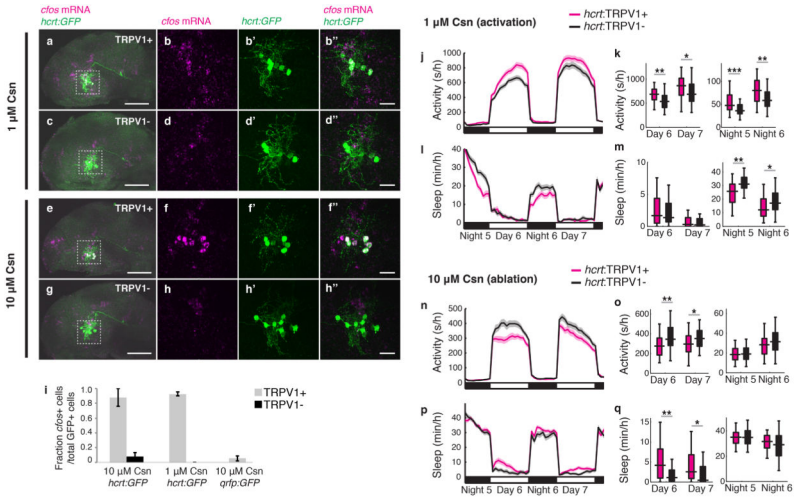

Figure 3. TRPV1–mediated activation and ablation of Hcrt neurons affects sleep–wake behaviors

(a–h) Representative images of Hcrt neurons (anti–EGFP IHC, green), and *c–fos* expression (FISH, magenta), in TRPV1^{+} (a,b,e,f) and TRPV1^{-} (c,d,g,h) larvae after incubation in 1 µM (a–d) or 10 µM (e–h) Csn for 20 minutes. Sagittal images of 3 dpf larval brains (a,c,e,g, scale = 100 µm) and magnified views of the boxed areas (b,d,f,h, scale = 20 µm) are oriented with rostral at left. Images are maximum intensity projections of 40 µm z–stacks. A gamma correction was uniformly applied across all images to visualize cells with lower signal. (i) Mean ± s.e.m. fraction of *c–fos*–positive cells for (a–h) and Supplementary Fig. 9g,h. See methods for number of samples. (j–m) Behavioral phenotypes during activation of Hcrt neurons with 1 µM Csn in *Tg(hcrt:TRPV1–RFPT)* larvae (n = 44) compared to WT siblings (n = 44). (n–q) Behavioral phenotypes following ablation of Hcrt neurons with 10 µM Csn in *Tg(hcrt:TRPV1–RFPT)* larvae (n = 52) compared to WT siblings (n = 43). Behavioral recording began on night five and ended on the night seven of development. Line plots indicate mean ± s.e.m. Box plots indicate median (solid black line), 25th and 75th percentiles (box) and data range (whiskers). *P<0.05, **P<0.01 and ***P<0.001 for transgenic larvae compared to their WT siblings by Wilcoxon rank–sum test.